

P54nr_b Forms a Heterodimer with PSP1 That Localizes to Paraspeckles in an RNA-dependent Manner[□] [▽]

Archa H. Fox,* Charles S. Bond,[†] and Angus I. Lamond*

*Division of Gene Regulation and Expression and [†]Division of Biological Chemistry and Molecular Microbiology, Wellcome Trust Biocentre, University of Dundee, Dundee DD1 5EH, United Kingdom

Submitted June 30, 2005; Revised August 24, 2005; Accepted August 25, 2005
Monitoring Editor: Joseph Gall

P54nr_b is a protein implicated in multiple nuclear processes whose specific functions may correlate with its presence at different nuclear locations. Here we characterize paraspeckles, a subnuclear domain containing p54nr_b and other RNA-binding proteins including PSP1, a protein with sequence similarity to p54nr_b that acts as a marker for paraspeckles. We show that PSP1 interacts in vivo with a subset of the total cellular pool of p54nr_b. We map the domain within PSP1 that is mediating this interaction and show it is required for the correct localization of PSP1 to paraspeckles. This interaction is necessary but not sufficient for paraspeckle targeting by PSP1, which also requires an RRM capable of RNA binding. Blocking the reinitiation of RNA Pol II transcription at the end of mitosis with DRB prevents paraspeckle formation, which recommences after removal of DRB, indicating that paraspeckle formation is dependent on RNA Polymerase II transcription. Thus paraspeckles are the sites where a subset of the total cellular pool of p54nr_b is targeted in a RNA Polymerase II-dependent manner.

INTRODUCTION

P54nr_b (NONO in mouse) has been implicated in numerous processes within the nucleus including transcriptional regulation, splicing, DNA unwinding, nuclear retention of hyperedited double-stranded RNA, viral RNA processing, control of cell proliferation, and circadian rhythm maintenance (Shav-Tal and Zipori, 2002; Brown *et al.*, 2005). P54nr_b is abundant and ubiquitous, can bind single- and double-stranded RNA and DNA and has inherent carbonic anhydrase activity. Originally, p54nr_b was purified as a heterodimer with PSF (Zhang *et al.*, 1993), a protein with extensive sequence homology to p54nr_b, and many reports have indicated p54nr_b and PSF copurify in the numerous nuclear complexes in which p54nr_b is found.

A major puzzle is how p54nr_b carries out all its disparate activities within the nucleus. It has been speculated that the phosphorylation status and intranuclear location of p54nr_b is critical in this (Shav-Tal and Zipori, 2002). We have previously reported an enrichment of p54nr_b in paraspeckles, a novel subnuclear compartment (Fox *et al.*, 2002). Paraspeckles were originally identified in HeLa cells but are also found in primary cells, other transformed cell lines, and tissue sections (Fox *et al.*, 2002). Mammalian cells contain typically 2–20 paraspeckles within the interchromatin space, usually in close proximity to splicing speckles. Paraspeckle Protein 1

(PSP1), is a marker for paraspeckles that shares sequence similarity with both p54nr_b and PSF (Fox *et al.*, 2002). PSP1 is usually accumulated in paraspeckles and diffusely distributed in the nucleoplasm. However, when RNA Polymerase (Pol) II transcription is inhibited by drug treatment, PSP1 leaves paraspeckles and accumulates at the nucleolus, concentrating in crescent-shaped structures termed “perinucleolar caps.” FLIP (fluorescence loss after photobleaching) shows that molecules of PSP1 are constantly trafficking between paraspeckles and nucleoli when transcription is active (Fox *et al.*, 2002). Similarly, the paraspeckle proteins PSP1 and p54nr_b are also found in the human nucleolar proteome (Andersen *et al.*, 2002) and p54nr_b accumulates at the same perinucleolar caps upon transcription inhibition. Beyond its presence in paraspeckles, little is known about the function of PSP1. At least two different isoforms, PSP1 α (the major isoform in HeLa cells, in this study referred to as “PSP1”) and PSP1 β , have been detected in mouse and human (Fox *et al.*, 2002; Myojin *et al.*, 2004) and may be tissue-specific (Myojin *et al.*, 2004).

P54nr_b, PSP1, and PSF share ~50% sequence identity; however, PSF has an additional large N-terminal domain that differentiates it from both PSP1 and p54nr_b. The major similarity resides in a so-called “DBHS” (*Drosophila* behavior and human splicing) domain, comprising two RRM motifs followed by a charged protein-protein interaction module. Consistent with a housekeeping role, all three proteins are ubiquitously expressed and are conserved in vertebrates. Invertebrate species such as *Drosophila melanogaster*, *Caenorhabditis elegans*, and mosquito only have one gene representing the p54nr_b/PSF/PSP1 family. In *D. melanogaster*, NONA, is involved in eye development and behavior (Jones and Rubin, 1990) and has a role in circadian rhythm maintenance, similar to p54nr_b (Brown *et al.*, 2005). In *Chironomus tentans*, the homolog is Hrp65, which is expressed as three isoforms (Miralles and Visa, 2001) and one of these, Hrp65-2, binds actin (Miralles *et al.*, 2000; Percipalle *et al.*, 2003). Hrp65 localizes to fibers that associate with nascent Balbiani ring

This article was published online ahead of print in *MBC in Press* (<http://www.molbiolcell.org/cgi/doi/10.1091/mbc.E05-06-0587>) on September 7, 2005.

[□] [▽] The online version of this article contains supplemental material at *MBC Online* (<http://www.molbiolcell.org>).

Address correspondence to: Angus I. Lamond (a.i.lamond@dundee.ac.uk).

Abbreviations used: Pol, polymerase; ActD, actinomycin D; IP, immunoprecipitation.

transcripts and self-associates through the C-terminal part of its DBHS domain (Kiesler *et al.*, 2003).

Besides PSP1 and p54nrb, two other RNA-binding proteins localize to paraspeckles in HeLa cells. First, PSP2 (SIP/CoAA), which also contains two RRM motifs and has been found in transcriptional corepression and coactivation complexes that modulate steroid receptor-dependent transcriptional regulation (Iwasaki *et al.*, 2001; Auboeuf *et al.*, 2004). Another link between the PSP1/PSF/p54nrb family and PSP2 is their mutual copurification in a search for Androgen receptor-binding proteins (Ishitani *et al.*, 2003). Finally, a factor involved in the first step in pre-mRNA 3'-end processing, CFI(m)68, was reported to accumulate within foci that partly colocalize with paraspeckles (Dettwiler *et al.*, 2004).

To characterize the paraspeckle localization of the p54nrb/PSP1/PSF family of proteins, we have analyzed paraspeckle formation and maintenance throughout the cell cycle. We find that PSP1 forms a novel heterodimer with p54nrb and is targeted to paraspeckles in a RNA-dependent manner, whereas its accumulation at perinucleolar caps does not require RNA.

MATERIALS AND METHODS

Cell Culture and Transfection

HeLa cells were grown in DMEM supplemented with 10% fetal calf serum (FCS) and 1% penicillin streptomycin (both Invitrogen, Carlsbad, CA). HeLa^{YFP-PSP1 α} (Fox *et al.*, 2002) were grown in DMEM as above with the addition of 200 μ g/ml G418 geneticin (Roche, Indianapolis, IN). Transfections were performed using the Qiagen Effectene reagent (Chatsworth, CA) according to the manufacturer's instructions. Typically, cells were analyzed 16–18 h post-transfection; however, only cells with low levels of expression were imaged, because overexpression of PSP1 and its derivatives causes mislocalization of the protein to nuclear aggregates. Drug treatments with actinomycin D (ActD; Sigma, St. Louis, MO) were carried out at a final concentration of 1 μ g/ml for 4 h.

Plasmid Production

Mutants of PSP1 were generated by PCR and cloned into PeYFP-C1 cut with *EcoRI* and *BamHI*, using restriction enzyme sites for *EcoRI* and *BamHI* engineered onto the 5' and 3' ends, respectively, of the PCR primers. Mutations in PSP1 α RNA-binding motifs (RRMs) were made by overlapping PCR using complementary oligonucleotides containing the base pair substitutions (F119A and F121A, K198A and F200A) in conjunction with primers for the 5' and 3' ends of PSP1 α (to generate full-length mutants) or primers for PSP1 residues 125–358 (to generate mutations in the minimal paraspeckle domain of PSP1). PA-GFP-PSP1 α was generated by excising PSP1 α from PeYFP-C1-PSP1 α (see Fox *et al.*, 2002) using *EcoRI* and *BamHI* and subcloning into PA-GFP-C1 (kind gift of J. Lippincott-Schwartz) cut with the same enzymes. PETDuet-1-6HisPSP1/p54nrb was made by PCR of PSP1 and p54nrb as follows: p54nrb (residues 80–313) was generated by PCR using primers with *NdeI* and *BglIII* sites at the 5' and 3' ends, respectively. The resultant product was then cloned into pETDUET-1 MCS2 cut with the same enzymes. Flag and thrombin tagged PSP1 was made by two-step PCR of PSP1 (residues 61–328) with a first step oligonucleotide pair that generated thrombin-cleavage-site-tagged-PSP1, and a second-step PCR that added a *BamHI* and Flag tag to the thrombin cleavage site. This was then cloned into the *BamHI* and *EcoRI* sites of MCS1 of pETDUET-1-p54nrb, keeping the translation frame the same as the vector to utilize the start methionine and His tag encoded upstream of MCS1. PeGFP-PSF was a kind gift of V. vanHeyningen.

Microscopy and Immunostaining of Live and Fixed Cells

For live-cell microscopy, HeLa^{YFP-PSP1 α} were seeded onto WillCo-glass-bottom dishes (Intracel, Rockville, MD) and incubated at 37°C, 5% CO₂. Approximately 1 h before imaging, the medium was replaced with CO₂-independent DMEM containing FCS and penicillin/streptomycin (Life Technologies, Rockville, MD) and the cells allowed to equilibrate at 37°C within the prewarmed environmental chamber (Solent Scientific, Segensworth, United Kingdom) fixed to the Zeiss DeltaVision restoration microscope (Thornwood, NY). Cells were imaged using a FITC filter fitted with a neutral density filter that removes 90% of the light, with a 63 \times NA 1.4 Plan-Apochromat objective lens with 2 \times 2 binning. For each time point, 24 sections at 0.5- μ m intervals were obtained through each cell, each with a 0.1-s exposure time. Experiment length was 2–16 h, with 2–4-min time points. To label DNA in live cells, they were preincubated with DMEM containing 0.15 μ g/ml bisbenzimidazole (Sigma)

for 30 min. This mixture was replaced with CO₂-independent medium, and the cells allowed to recover for 30 min before imaging as described above. To see the bisbenzimidazole signal, fluorescence was captured using DAPI filter sets and 0.1-s exposures. To look at the effect of the transcription inhibitor DRB, the drug was diluted into CO₂-independent DMEM (final concentration 20 μ g/ml) and added to the cells.

For nuclease digestion experiments, HeLa^{YFP-PSP1 α} cells were grown on coverslips, rinsed briefly in phosphate-buffered saline (PBS), and then rinsed in permeabilization buffer (20 mM Tris-HCl, pH 7.4, 5 mM MgCl₂, 0.5 mM EGTA, protease inhibitor; Roche). Cells were then permeabilized for 5 min at room temperature in permeabilization buffer (as above) containing 0.05% Triton X-100. Coverslips were rinsed three times in permeabilization buffer and then incubated with RNase A (Sigma, 100 μ g/ml in PBS) or DNase (Worthington, Lakewood, NJ; 100 μ g/ml in PBS + 5 mM MgCl₂) for 20 min at room temperature. After nuclease degradation, cells were rinsed in PBS and then fixed, stained with DAPI and pyronin Y to monitor the success of the nuclease digestion, mounted onto slides, and imaged as described below.

For imaging fixed cells, cells were grown on coverslips, rinsed in PBS, and fixed for 5 min at room temperature in 4% paraformaldehyde in CSK buffer (10 mM pipes, pH 6.8, 100 mM NaCl, 300 mM sucrose, 3 mM MgCl₂, and 2 mM EDTA). After permeabilization (1% Triton X-100 [sigma] in PBS for 15 min at room temperature), immunofluorescence labeling was carried out as previously described (Fox *et al.*, 2002). Antibodies used were rabbit anti-PSP1 (dilution 1:50; Fox *et al.*, 2002), rabbit anti-PSP1_48 (dilution 1:500, this study), monoclonal B92 anti-PSF (Sigma), anti-rabbit TRITC-conjugated secondary antibody (Jackson ImmunoResearch Laboratories, West Grove, PA; 1:250), anti-mouse TRITC-conjugated secondary antibody (Jackson, 1:250), anti-mouse Cy5-conjugated secondary antibody. Before mounting cells were stained with DAPI (0.3 μ g/ml, Sigma) for 1 min and then mounted using Vectashield (Vector Laboratories, Burlingame, CA).

Immunoprecipitation and Immunoblotting

For immunoprecipitation (IP) with anti-PSP1 antiserum, 150 μ l (bead volume) recombinant protein A Sepharose (Amersham, Piscataway, NJ) was rinsed in TN buffer (150 mM Tris, pH 7.4, 20 mM NaCl, 0.01% NP40) and then added to antibody solution (65 μ g antibody in 150 μ l TN buffer) and incubated with shaking overnight at 4°C. Antibodies used were anti-PSP1 (Ab1; Fox *et al.*, 2002), anti-PSP1_48 (Ab2, this study), or rabbit preimmune serum. Washed, antibody-loaded beads were then incubated with either 300 μ l commercial HeLa nuclear extract (~5 mg/ml, CIL Biotech, Belgium) or HeLa nuclear lysate made from cells cultured in-house (cultured either in the absence or presence of ActD for 4 h). Nuclear lysates were made by lysing cells in 50 mM Tris, pH 7.5, 0.5M NaCl, 1% NP40, 1% DOC, 0.1% SDS, 2 mM EDTA with complete protease inhibitors, followed by shearing of the DNA in a Qias shredder (Qiagen). Reactions were shaken for 2 h at 4°C, the supernatant was removed, and the beads were rinsed three times with 1 ml TN buffer. SDS loading buffer was then added to the beads and samples of supernatants and the proteins were subjected to SDS-PAGE, followed in some cases by Western blotting and in other cases by Colloidal Blue staining (Novex, Encinitas, CA). Some IPs were also subjected to high stringency washes in Tris (pH 7.4) and either 0.4, 0.7, or 1 M NaCl in conjunction with either 0.05, 1, or 2% NP40. For experiments where cognate complexes were specifically eluted off the beads using cognate peptides, the rinsed beads, with IP bound, were split into two and placed into Amicon UltraFree-MC centrifugal filter devices (Millipore, Beverly, MA). TN buffer, 30 μ l, containing either 10 μ g peptide or no peptide was then added to each. After 5-min incubation at RT, the eluate was spun through the column and reloaded, incubated again for 5 min, and finally spun and collected. Eluted complexes or washed beads were then subjected to SDS-PAGE and stained with either Colloidal Blue (Novex) or silver-stained. IP with anti-GFP were performed essentially as described above, except on a smaller scale, with mouse anti-GFP (Roche) incubated with protein G Sepharose (Amersham) overnight at 4°C. Nuclear lysates were prepared from HeLa cells transfected 16–18 h earlier with plasmids expressing YFP and YFP fusion proteins and incubated with antibody-bound beads for 2 h at 4°C. Mass spectrometry was carried out by the Fingerprints Facility, University of Dundee.

Western blotting was carried out on proteins transferred to Hybond C nitrocellulose (Amersham) using either anti-PSP1_48 (Ab2, rabbit polyclonal, 1:5000) or anti-p54nrb (mouse monoclonal, Transduction Laboratories, Lexington, KY; 1:5000) followed by incubation with anti-rabbit or anti-mouse peroxidase-coupled secondary antibodies (Pierce, Rockford, IL) and detection with ECL plus chemiluminescence (Amersham).

Recombinant Protein Production

PETDUET-1-His₆-PSP1/p54nrb was transformed into *E. coli* (Rosetta-gami(DE3)pLysS; Novagen, Madison, WI). Bacteria were induced overnight at RT with 2 mM IPTG and then lysed in 20 mM Tris, pH 7.5, 200 mM NaCl, 5 mM imidazole using a one-shot cell disrupter (Constant Cell Disruption Systems). The lysate was loaded onto a His-trap column (Amersham), washed, and fast-performance liquid chromatography (FPLC) was performed (BioCad700E, Global Medical Instruments, Ramsey, MN) with a 50–500 mM imidazole gradient to elute the complex. The peak fractions were concen-

trated to 2 ml volume and then loaded onto a superdex200 column (Amersham) preequilibrated with 150 mM NaCl, 20 mM Tris, pH 7.5, 1 mM DTT. FPLC was performed according to the manufacturer's instructions (AKTA; Amersham) and the peak fractions were collected.

PSP1 Dynamics

HeLa cells, transfected with PA-GFP-PSP1 α plasmid, were grown and imaged as described for "live cell microscopy" above. Eighteen hours posttransfection, the dish of cells was placed in the chamber fitted to an Olympus DeltaVision restoration microscope (Applied Precision, Issaquah, WA) fitted with a 406-nm laser. Using a 63 \times objective (NA of 1.4) cells were scanned for low levels of expression of PA-GFP-PSP1 using a standard fluorescence mercury lamp and a FITC filter. Selected cells were then activated by a 0.5-s 406-nm laser pulse focused to a diffraction-limited spot of $\sim 1.5\text{-}\mu\text{m}$ diameter by the objective lens. A single z-section through the activated region of each cell was imaged using a FITC filter, both before the laser pulse, as well as afterward with an iterative time-course for a 35-s period. These cells were marked in a point list so that they could be revisited after incubation with the drug, ActD, and the experiment could be repeated on the perinucleolar cap structures formed as a result of this treatment. In total, 30 cells were imaged this way. The fluorescence intensity of the photoactivated spot was recorded for each time point (Softworx, edit polygon function, Applied Precision). The fluorescence recorded before activation was subtracted as background, and the resulting values converted to a ratio of fluorescence intensity, whereby the fluorescence recorded at each time point was divisible by the first fluorescence reading after activation by the laser. These data were then graphed against time. Half-lives were determined by two-phase exponential decay curve fitting using Prism4 software (Graphpad, San Diego, CA).

RESULTS

Paraspeckles in the Cell Cycle

The localization and behavior of paraspeckles through the cell cycle was characterized by time-lapse fluorescence imaging of a stable HeLa cell line (HeLa^{YFP-PSP1 α}) expressing the paraspeckle marker protein, YFP-PSP1 (Figure 1, and the Supplementary Video1.mov). This stable cell line progresses through mitosis at a rate similar to the parental HeLa cells, and the YFP-PSP1 fusion is expressed at low levels reflecting the properties of endogenous PSP1 (Fox *et al.*, 2002). Time-lapse data show that paraspeckles persist throughout interphase and during most of mitosis, including prophase, metaphase, and anaphase (Figure 1A, paraspeckles shown by arrows). This contrasts with the behavior of many other nuclear bodies, including nucleoli and Cajal bodies, which disassemble when cells enter mitosis (Carmo-Fonseca *et al.*, 1993; Bubulya *et al.*, 2004; Leung *et al.*, 2004). Further, paraspeckles seen in mitotic cells are not associated with condensed chromatin (Figure 1B). In telophase, when daughter nuclei form, paraspeckles are not initially detected in the nucleoplasm. Instead the cytoplasmic paraspeckles disappear and the YFP-PSP1 protein enters the nucleus and predominantly localizes to several perinucleolar caps (Figure 1A, arrowheads). Comparison of these YFP-PSP1 telophase structures with DIC images confirmed these colocalized with newly formed nucleoli (Figure 1C). A time course of a representative cell completing mitosis reveals the appearance of perinucleolar YFP-PSP1 20–30 min after metaphase (Supplementary Figure 1). The perinucleolar caps persist for 20–30 min, after which the YFP-PSP1 signal becomes diffuse in the nucleoplasm. After a further 60–90 min individual paraspeckles begin to appear (Supplementary Figure 1).

The accumulation of YFP-PSP1 in perinucleolar caps during telophase is reminiscent of the PSP1 perinucleolar caps that form upon treatment of cells in interphase with drugs that inhibit RNA Pol II transcription (Fox *et al.*, 2002). RNA Pol II transcription does not commence immediately upon the formation of daughter nuclei, as defined by the formation of the nuclear envelope (Prasanth *et al.*, 2003). Thus, YFP-PSP1 may accumulate within perinucleolar caps during

telophase because at this stage there is little or no RNA Pol II transcription in the daughter nuclei. To test this, we treated mitotic HeLa^{YFP-PSP1 α} cells with DRB, a drug that reversibly inhibits RNA Pol II transcription (Figure 2, Supplementary Video2.mov). In the presence of DRB, YFP-PSP1 still accumulated at perinucleolar caps ~ 30 min after metaphase (Figure 2, 00:37 time-point, arrowheads show perinucleolar PSP1). However, these perinucleolar caps were no longer transient and persisted for as long as the drug was in the culture medium (Figure 2). This effect is reversible, as shown by the YFP-PSP1 signal becoming diffuse in the nucleoplasm 90–120 min after washing DRB out of the culture medium (Figure 2, time point 01:22 and later). Quantifying the total nuclear fluorescence shows no apparent change in YFP-PSP1 signal before and after DRB treatment, indicating that the changing localization observed is due to a redistribution of PSP1 from perinucleolar caps to the nucleoplasm, rather than protein degradation. Paraspeckles subsequently reappear in the nucleoplasm after a further lag of 90–120 min (Figure 2, 06:10, arrows). This is the same time taken for reappearance of paraspeckles in untreated cells after dispersal of the telophase perinucleolar caps. A likely explanation for the lag in reforming paraspeckles in the nucleoplasm of daughter nuclei is that paraspeckle formation may depend on the accumulation of RNA Pol II transcripts and/or their downstream products.

The Role of RNA in Paraspeckle Structure

The apparent requirement for RNA Pol II transcripts to form paraspeckles suggests that they may contain RNA. To test whether RNA is required for paraspeckle integrity, HeLa^{YFP-PSP1 α} cells were permeabilized, treated with RNase A and the location of YFP-PSP1 examined in the fluorescence microscope; the typical pattern of paraspeckles is no longer detected in cells following RNase treatment (Figure 3, compare A and B, arrows show paraspeckles in green). The absence of Pyronin Y staining, a dye that labels total RNA, was used to confirm the efficacy of the RNase A treatment (unpublished data). A similar result was obtained with the parental HeLa cells using an anti-PSP1 antibody to detect endogenous PSP1 (unpublished data). The RNase experiment was repeated using cells treated with ActD, where PSP1 had relocated to perinucleolar caps; in this case the RNase treatment did not remove the PSP1 signal in perinucleolar caps (Figure 3, C and D, arrowheads indicate perinucleolar caps). RNase A was equally effective at degrading RNA in both control and ActD-treated cells, as judged by the disappearance of total cellular RNA signal (Pyronin Y signal, unpublished data). This RNase A experiment suggests that different interactions may be involved in retaining PSP1 at paraspeckles and perinucleolar caps, respectively.

Paraspeckles were observed to be clearly separate from the condensed chromosomes in mitotic cells (Figure 1B), indicating that DNA is not required for paraspeckle stability during cell division. This is also the case for interphase cells as DNase I digestion of both control and ActD-treated cells in interphase showed no change in the pattern of PSP1 labeling (unpublished data). These data support the view that specifically RNA is important for PSP1 localization to paraspeckles.

The Minimal Domains of PSP1 Required for Paraspeckle and Perinucleolar Cap Localization

Because all known paraspeckle proteins contain RNA-binding motifs, we next tested whether the ability of PSP1 to bind RNA was important for paraspeckle localization. The local-

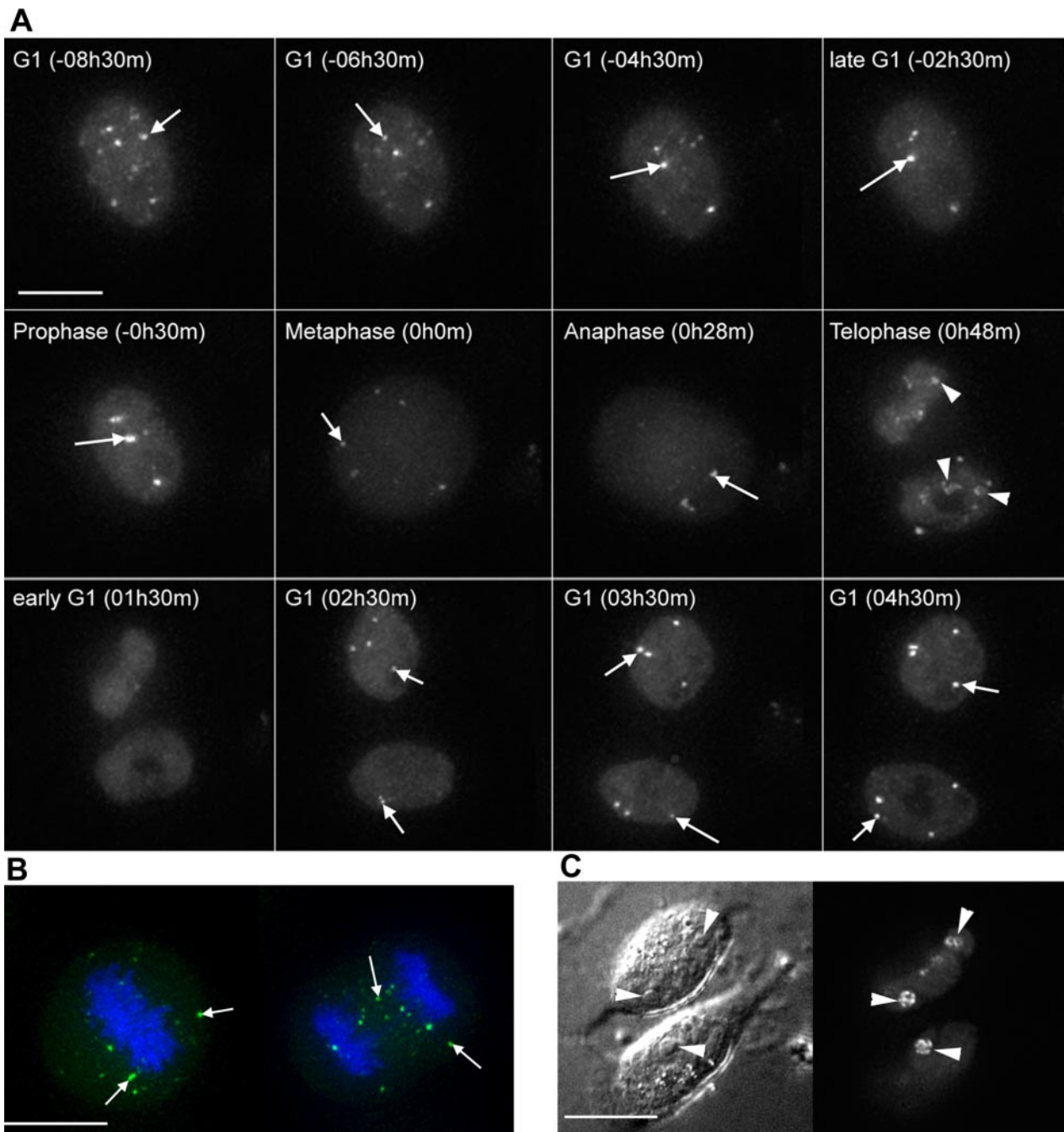


Figure 1. Paraspeckles through the cell cycle. (A) Fluorescent micrographs of a HeLa^{YFP-PSP1 α} cell acquired over the course of 16 h of live-cell imaging (see *Materials and Methods*). For movie see Supplementary Video1.mov. (B) Fluorescent micrographs of a representative live HeLa^{YFP-PSP1 α} cell (YFP-PSP1, green signal) treated with bisbenzamide to label DNA (Blue signal), before imaging through mitosis. (C) DIC and fluorescence image of a HeLa^{YFP-PSP1 α} cell at telophase, acquired as part of a live-cell time-course imaging experiment. Scale bar, 10 μ m. Arrows, paraspeckles; arrowheads, perinucleolar caps.

ization of a series of truncated and mutated forms of YFP-tagged PSP1 was analyzed after transient transfection into HeLa cells (Figure 4). PSP1 constructs lacking either the N-terminus (residues 1–80, unpublished data), the C-terminus (359–523, mutant A) or both termini (mutant D) still localize to paraspeckles. These data are consistent with the previous report that PSP1 β , a minor PSP1 isoform in HeLa cells that only shares residues 1–387 with PSP1 α , also localizes to paraspeckles (Fox *et al.*, 2002).

We next explored the effect of further deletions to remove either one or both of the RRM RNA-binding motifs (residues 81–150 and 155–230, respectively) or the coiled coil domain (residues 287–358). The minimal region of PSP1 that accumulated in paraspeckles contained only the RRM2 RNA-binding domain and the coiled coil domain (mutant G, residues 125–358). However neither the RRM domains alone (mutant B) nor the coiled coil domain alone (mutant F) were sufficient for paraspeckle localization.

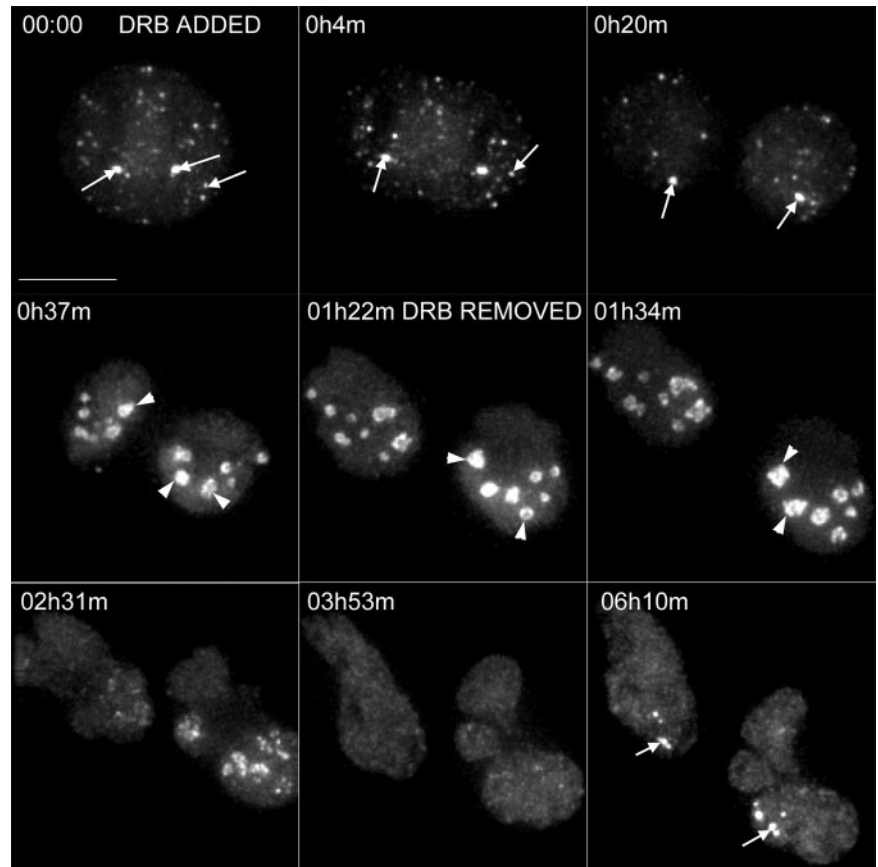


Figure 2. Transcription inhibition by DRB treatment prolongs the appearance of perinucleolar YFP-PSP1 in newly divided cells, with paraspeckles only forming once the drug is removed. A panel of fluorescent micrographs acquired by live-cell imaging HeLa^{YFP-PSP1 α} cells every 3 min over the course of 7 h. At the start of the experiment, after cell division, DRB was added, and then removed, in this case, 1 h 22 min after cell division. Scale bar, 10 μ m. Arrows, paraspeckles; arrowheads, perinucleolar caps. See Supplementary Video2.mov for movie.

Next, we addressed whether the requirement for an RRM domain was due to its RNA-binding activity. Mutations that abolish RNA binding without disrupting the overall structure of the RRM domain were made in both RRMs of PSP1 (F119A and F121A in RRM1 and K198A and F200A in RRM2; Serin *et al.*, 1997; Lisbin *et al.*, 2000). Abolishing the RNA-binding ability of either RRM (leaving the other RRM intact) did not prevent full-length PSP1 from accumulating in paraspeckles (Figure 4, mutants H and I), indicating that either RRM motif can fulfil the RNA binding activity required for paraspeckle localization. However, when both RRM motifs were mutated or when RRM2 in the minimal paraspeckle-localized PSP1 fragment was mutated, the resulting mutants no longer accumulated in paraspeckles (mutants J and K). Thus, we infer that PSP1 requires the ability to bind RNA via an RRM domain in order to localize to paraspeckles. As the coiled coil domain is also required, we conclude that a functional RRM is necessary but not sufficient for paraspeckle localization of PSP1.

We next investigated which domains in PSP1 are required for it to accumulate at perinucleolar caps upon inhibition of RNA Pol II transcription. The same series of mutant PSP1 constructs were transiently expressed after transfection into HeLa cells, which were subsequently treated with ActD (1 μ g/ml) for 4 h (Figure 4 for summary, Supplementary Figure 2 for fluorescence micrographs). Again, the extreme N and C termini of the protein were not required for cap localization (mutants D and A). However, in contrast to the requirement for paraspeckle localization, deletion of either one, or both, RRM domains did not prevent cap localization (mutants C, F, and G). The minimal region of PSP1 that could still localize to perinucleolar caps contained the entire

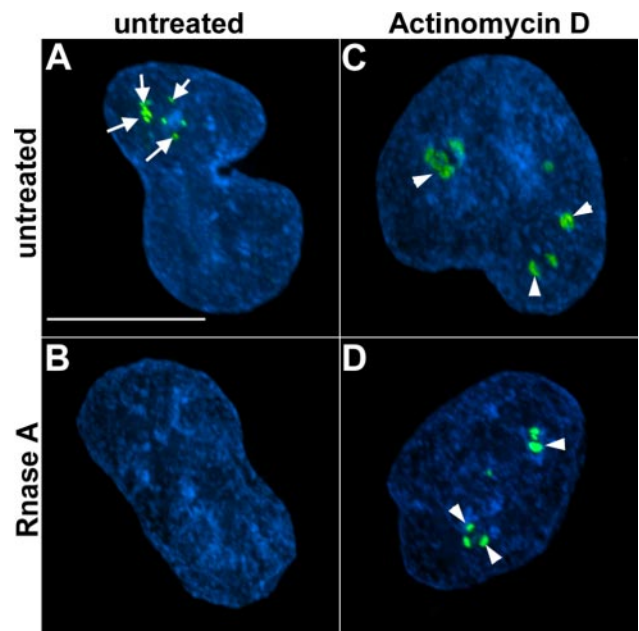


Figure 3. RNase A treatment abolishes YFP-PSP1 α signal in paraspeckles, but not peri-nucleolar caps. Fluorescent micrographs of a representative HeLa^{YFP-PSP1 α} cell (A and B) and a HeLa^{YFP-PSP1 α} cell that was pretreated with ActD (C and D) following incubation with either buffer (A and C), or buffer containing RNase A (B and D). Blue, DAPI; green, YFP-PSP1. The absence of Pyronin Y staining was used to confirm the efficacy of the RNase A treatment (unpublished data). Scale bar, 10 μ m. Arrows, paraspeckles; arrowheads, perinucleolar caps.

					para- speckles?	caps?
YFP-PSP1-1-1-523	RRM1	RRM2	coiled coil		+	+
mutant A (YFP-PSP1-1-358)	RRM1	RRM2	coiled coil		+	+
mutant B (YFP-PSP1-1-235)	RRM1	RRM2			-	-
mutant C (YFP-PSP1-236-523)			coiled coil		-	+
mutant D (YFP-PSP1-81-358)	RRM1	RRM2	coiled coil		+	+
mutant E (YFP-PSP1-81-286)	RRM1	RRM2			-	-
mutant F (YFP-PSP1-231-358)			coiled coil		-	+
mutant G (YFP-PSP1-125-358)		RRM2	coiled coil		+	+
mutant H (YFP-PSP1-RRM1mut)	RRM1	RRM2	coiled coil		+	+
mutant I (YFP-PSP1-RRM2mut)	RRM1	RRM2	coiled coil		+	+
mutant J (YFP-PSP1-doublemut)	RRM1	RRM2	coiled coil		-	+
mutant K (YFP-PSP1-125-358mut)		RRM2	coiled coil		-	+

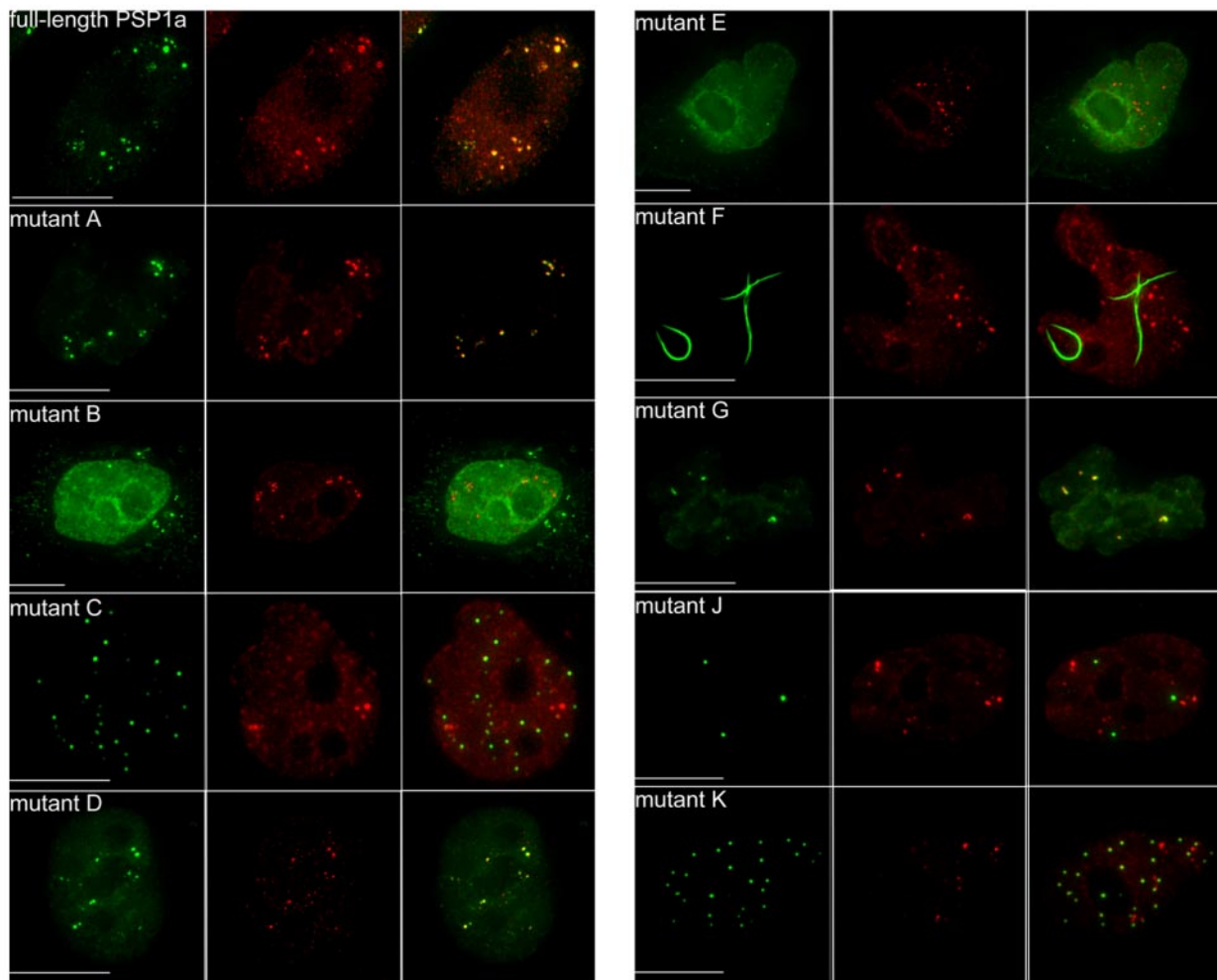


Figure 4. Regions of PSP1 required for localization to paraspeckles and perinucleolar caps. The top panel shows a summary of the localization pattern of YFP-fusions of PSP1 mutants expressed in HeLa cells. Below, representative fluorescence micrographs of a subset of the YFP-PSP1 mutants expressed in HeLa (green signal) and immunostained with a paraspeckle marker (red signal) that was either PSP1 (PSP1 Ab2 for mutants A, B, D, E, F, G, and K), or PSF (monoclonal B92, YFP-PSP1 and mutants C and H). The choice of paraspeckle marker was dictated by the location of the peptide epitope the PSP1 Ab2 was raised against (at the extreme C terminus of PSP1); therefore any PSP1 mutant that contained this region could not be compared with endogenous PSP1 due to antibody cross-reactivity with the overexpressed fusion proteins. Representative fluorescent micrographs of mutant localization patterns following ActD treatment are shown in Supplementary Figure 2. Scale bars, 10 μ m. "Paraspeckle" localization is defined as the formation of multiple nucleoplasmic foci colocalizing with a paraspeckle marker protein with a fluorescence intensity quantitatively more than twice the background nucleoplasmic signal. "cap" localization is defined as the presence of perinucleolar caps after treatment of transfected cells with ActD (1 μ g/ml) for 4 h. Amino acid substitution mutations are indicated by an \times and are F119A, F121A (for RRM1) and K198A, F200A (for RRM2).

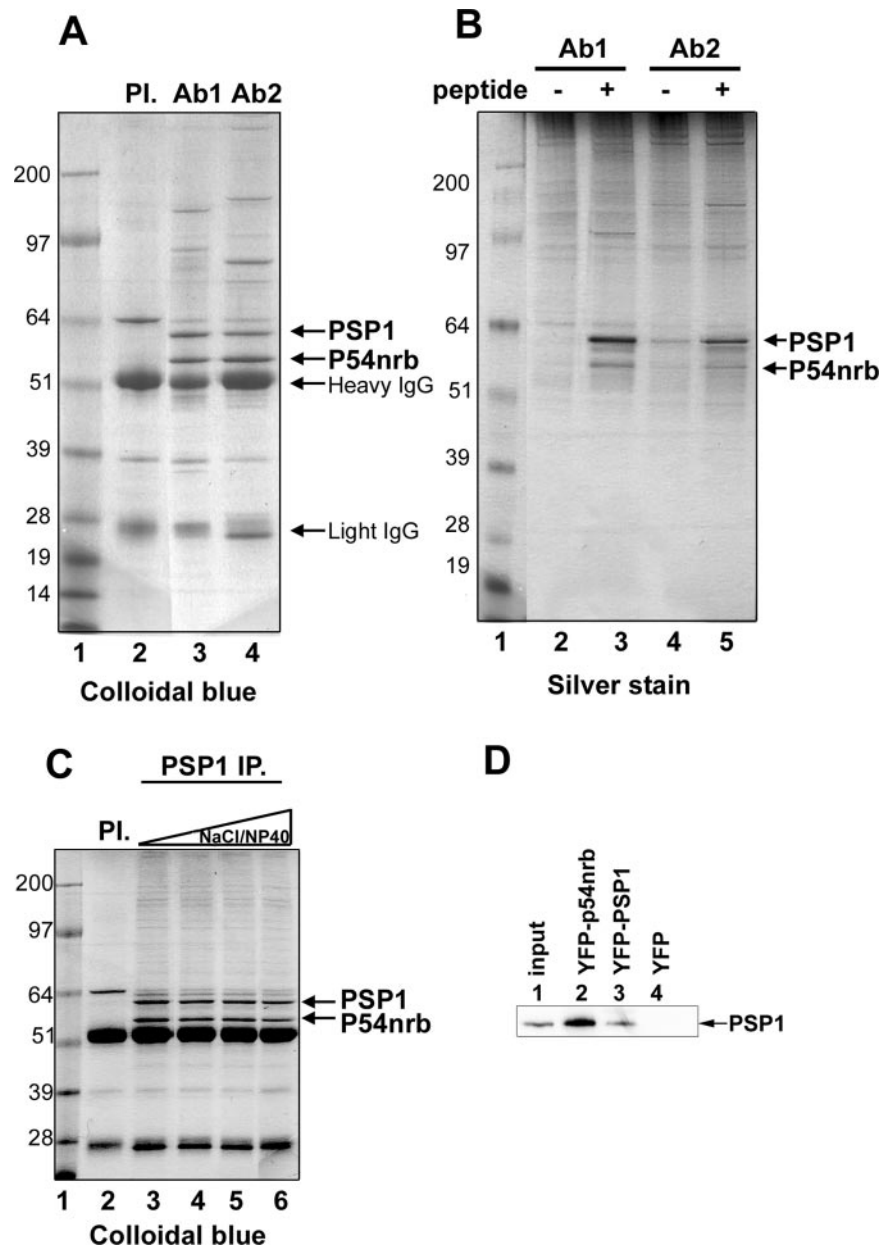


Figure 5. PSP1 associates with p54nrb in vivo. (A) Endogenous PSP1 was immunoprecipitated from HeLa nuclear extract using two different PSP1 antibodies (preimmune, lane 2; Ab1, lane 3; and Ab2, lane 4). The IP proteins were run on a 4–12% SDS-PAGE and stained with colloidal blue. (B) To elute specific PSP1 complexes, IP-bound beads were incubated with buffer (lanes 2 and 4), or the cognate peptide that each antibody was raised against (Ab1 peptide, lane 3 and Ab2 peptide, lane 5). The supernatant was subjected to SDS-PAGE, and the gel silver-stained. (C) IP PSP1 complex (using Ab2) was repeatedly washed with 0.1–1 M NaCl/0.1–2% NP40 (see *Materials and Methods*). The bound proteins were subjected to SDS-PAGE and stained with colloidal blue. In all panels, molecular weight markers are shown in lane 1 (kDa). (D) IP with anti-GFP antibodies using HeLa whole cell lysates transiently expressing either YFP-p54nrb (lane 2), YFP-PSP1 (lane 3), or YFP (lane 4). The resultant bound proteins were separated by SDS-PAGE and immunoblotted with anti-PSP1 antibody. “input” (lane 1) is HeLa whole cell lysate.

coiled coil domain, but neither of the RNA-binding domains (mutant F, residues 231–358). We note that this mutant forms extended, fibrous nuclear aggregates, in addition to the perinucleolar localization, presumably because of unregulated self-interaction of the coiled coil domain (Figure 4, mutant F). Comparison of mutants A and B shows that the deletion of the coiled coil domain prevents the localization of mutant B to perinucleolar caps, although it retains both RRM domains. We infer that the coiled coil domain is necessary and likely sufficient for the perinucleolar cap localization of PSP1.

PSP1 Interacts with p54nrb

Because it is likely that the coiled coil domain of PSP1 mediates protein-protein interaction, we next searched for proteins binding to endogenous PSP1. Thus coimmunoprecipitation (co-IP) of PSP1 was performed using two separate

anti-PSP1-peptide antibodies to pull out PSP1 binding partners from HeLa nuclear extract (Figure 5). The first antibody (Ab1, Fox *et al.*, 2002) raised against a peptide from the N-terminus of PSP1 and a second antibody (Ab2, this work), raised against a peptide in the C-terminus of PSP1, both specifically recognize PSP1 in HeLa cell extracts and show a typical paraspeckle staining pattern by immunofluorescence (sample Ab2 staining, see Figure 7B). HeLa nuclear extracts were incubated with beads coated either with preimmune serum, Ab1 or Ab2 and the specifically bound proteins eluted and separated by SDS-PAGE (Figure 5A). This showed two major bands common to both antibodies but absent from the preimmune control. (Figure 5A, arrows, cf. lanes 2 and 3 with lane 1). Both bands were also seen after selective elution from the antibody beads by addition of the cognate PSP1 peptides (Figure 5B). MALDI Mass Spectrometric analysis identified the upper band as PSP1 and the

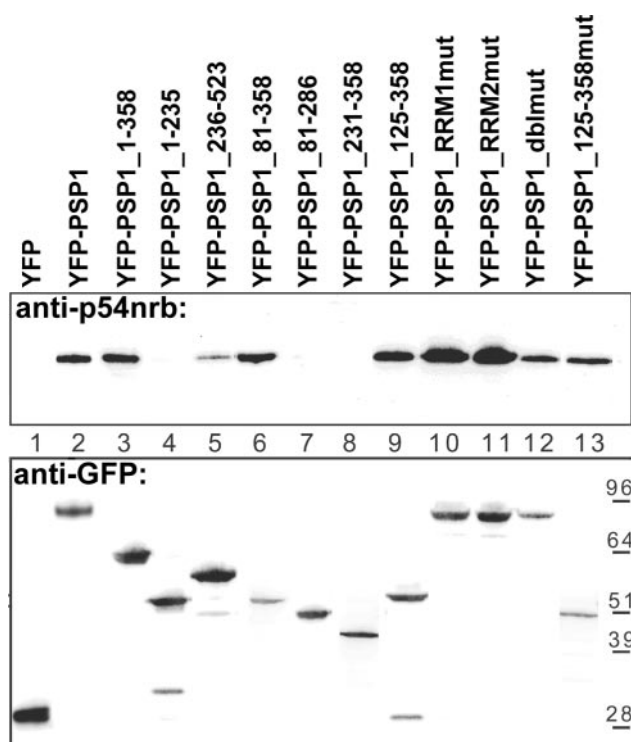


Figure 6. PSP1 requires its coiled coil domain to pull down p54nrbl. Whole cell lysates of cells transiently expressing either YFP (lane 1), YFP-PSP1 α (lane 2), or mutations in YFP-PSP1 α (lanes 3–13) were used for IP with anti-GFP antibody-cross-linked beads. The resultant bound proteins were then subjected to SDS-PAGE, transferred to nitrocellulose and immunoblotted with p54nrbl mAb (top panel), or GFP mAb (bottom panel), using ECL plus to visualize the signal.

lower band as p54nrbl. Despite the sequence similarity between PSP1 and p54nrbl, Western blot analysis of HeLa nuclear extract using both Ab1 and Ab2 at high concentrations shows no cross-reactivity of p54nrbl (unpublished data). In addition, the peptide epitope for Ab1 is in a region of PSP1 with no sequence similarity to p54nrbl. Thus we conclude that p54nrbl is able to co-IP as a result of its presence in vivo in a common complex with PSP1.

The association between PSP1 and p54nrbl is stable as well as specific, because increasing the stringency of washing the beads (up to 1 M NaCl/2% NP40 detergent) after IP did not disrupt the complex or change the apparent stoichiometry (Figure 5C). Similarly, treatment with RNase A did not disrupt the association (unpublished data). To test if p54nrbl can co-IP PSP1, we expressed YFP-p54nrbl in HeLa cells and used anti-GFP-bound beads to pull out the fusion protein and any bound cofactors (Figure 5D). Immunoblotting the IP with anti-PSP1 demonstrated that PSP1 was selectively co-IPed by YFP-p54nrbl (Figure 5D, lane 2), but not by YFP alone (lane 4). Interestingly, overexpressed YFP-PSP1 was also able to co-IP endogenous PSP1, although to a lesser extent than YFP-p54nrbl (Figure 5D, compares lanes 2 and 3).

We next determined which regions of PSP1 were required for the association with p54nrbl. The same series of truncated and mutated YFP-PSP1 constructs that were used in the localization studies above (Figure 4) were transiently expressed and assayed for co-IP of p54nrbl, using an anti-GFP antibody (Figure 6). P54nrbl could only co-IP with fragments of PSP1 containing the coiled coil domain (residues 231–

358). For example, PSP1 mutant G (125–358) binds p54nrbl (lane 9), yet PSP1 mutant B (1–235), which contains both RRM motifs, did not co-IP p54nrbl (lane 4). However, a PSP1 fragment containing the coiled coil region alone (mutant F, 231–358) also did not co-IP p54nrbl. We presume this results from the biophysical properties of the nuclear aggregates that form when this coiled coil domain is expressed without the normal flanking sequences (see Figure 4). We note that those constructs containing at least one RRM appear to pull down more p54nrbl than those without (Figure 6, compare mutants C and D). It is possible that one or both of the PSP1 RRM motifs (located within residues 81–235) are stabilizing the interaction of the coiled coil region with p54nrbl, because some RRM motifs are known to be involved in protein-protein contacts (Price *et al.*, 1998; Fribourg *et al.*, 2003; Selenko *et al.*, 2003). However, the RNA-binding function of the PSP1 RRM motifs is not required for p54nrbl interaction, because mutations within either one, or both of the PSP1 RRM motifs that abrogate its ability to bind RNA do not prevent co-IP of p54nrbl (Figure 6, lanes 12 and 13).

PSF Localizes to Paraspeckles

The minimal domains of PSP1 needed for paraspeckle and nucleolar cap localization (determined above) are common to the related nuclear RNA-binding protein PSF. We therefore examined the localization pattern of PSF using HeLa^{YFP-PSP1 α} cells immunolabeled with an anti-PSF monoclonal antibody (mAb). This showed PSF enriched in paraspeckles, as judged by colocalization with YFP-PSP1, with an additional diffuse PSF nucleoplasmic labeling (Figure 7A, arrows show paraspeckles). Exogenously expressed GFP-PSF also colocalized with paraspeckles, as judged by double labeling using an anti-PSP1 antibody (Figure 7B). It has previously been reported that PSF accumulates in perinucleolar caps after treatment of cells with transcription inhibiting drugs (Dye and Patton, 2001; Shav-Tal *et al.*, 2005). Double-labeling HeLa^{YFP-PSP1 α} cells with anti-PSF antibodies after treatment with ActD (Figure 7C, arrowheads show perinucleolar caps) showed that both YFP-PSP1 and PSF colocalized in the same perinucleolar caps. Similarly, GFP-PSF and endogenous PSP1 also colocalized in perinucleolar caps (Figure 7D).

PSP1 and p54nrbl Heterodimerize In Vitro

Despite this similarity in domain structure and in vivo localization properties between PSP1, p54nrbl, and PSF, the parallel biochemical analyses demonstrated that the predominant in vivo interaction of PSP1 was in a stoichiometric complex specifically with p54nrbl and not with PSF (see Figure 5 and other unpublished data). The association between PSP1 and p54nrbl was detected in extracts prepared from both transcriptionally active HeLa cells and extracts prepared after treatment with ActD (Figure 8A). This shows that PSP1 can co-IP p54nrbl at similar levels from both the control and ActD-treated cell extracts (Figure 8A, compare lanes 6 and 8). Further, these blotting data demonstrate that only a minor fraction of the total cellular pool of p54nrbl is able to co-IP together with PSP1, consistent with the fact that p54nrbl is expressed at higher levels than PSP1 (Figure 8A, lanes 1–4). In contrast, the absence of PSP1 remaining in the extract after IP shows that the anti-PSP1 antibody quantitatively depletes PSP1 (Figure 8A, compare levels of PSP1 in lanes 2 and 4 with 6 and 8). We conclude that PSP1 forms a complex with a subset of the total cellular pool of p54nrbl.

Finally, we tested whether fragments of PSP1 and p54nrbl containing their DBHS domains would be sufficient to promote direct interaction between the proteins. Both His₆-tagged PSP1 residues 61–328 and untagged p54nrbl residues

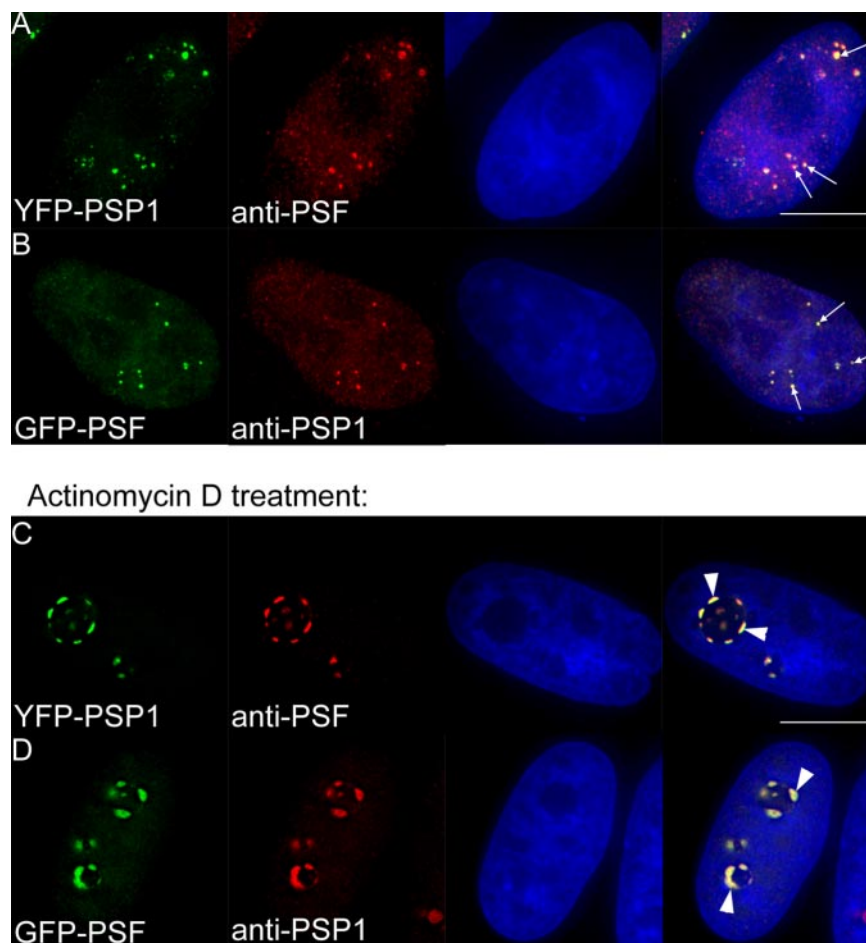


Figure 7. PSF localizes to paraspeckles. The panels show fluorescence micrographs of HeLa ^{YFP-PSP1α} cells (YFP fluorescence is green signal; A and C), or HeLa cells transiently expressing GFP-PSF (GFP fluorescence is green signal; B and D). Top panels (A and B) are untreated cells and bottom panels are cells incubated with ActD (C and D; see *Materials and Methods*). In each case, cells were immunostained with anti-PSF (red signal; A and C), or anti-PSP1 (red signal; B and D). Arrows, paraspeckles; arrowheads, perinucleolar caps. Blue signal is DAPI staining in all panels. Scale bar, 10 μ m.

75–313 were coexpressed in *E. coli* from a polycistronic plasmid vector. This showed stoichiometric copurification of the untagged p54nrb fragment upon affinity selection on Ni agarose and gel filtration chromatography to purify the His₆-tagged PSP1 fragment (Figure 8B). The major peak from the gel filtration chromatography indicated that the proteins form a stable heterodimer (unpublished data).

GFP-PSP1 Dynamics Differ at Paraspeckles and Perinucleolar Caps

Having established that PSP1 forms a stable complex with p54nrb regardless of the transcriptional status of the cell, we next tested whether any difference could be observed in the properties of PSP1 *in vivo* at either the paraspeckle or perinucleolar cap locations. To do this, we analyzed the dynamic behavior of PSP1 at both paraspeckles and caps by photoactivation of PAGFP-PSP1 that was transiently expressed in HeLa cells either with or without ActD treatment (Figure 9). Minimal regions of the live cell nucleus containing a single paraspeckle were activated by a 0.5-s laser pulse and the subsequent levels of activated fluorescence were measured at specified intervals for up to 35 s (see *Materials and Methods*). The cells were marked in a point-list and then reexamined after a 4-h incubation with ActD. The photoactivation experiment was then repeated, using the same conditions, on a single perinucleolar cap in each cell. Subsequent quantitation of fluorescence levels within the region of interest were plotted against time (Figure 9). This shows that the rate of movement of photoactivated PAGFP-PSP1 out of

perinucleolar caps is greater than out of paraspeckles (average half-lives of 14 and 31 s, respectively, $p < 0.0001$), suggesting that PSP1 has different molecular interactions and/or functions at these two distinct sites. It is possible that the slower movement of PSP1 out of paraspeckles is caused, at least in part, by the additional interaction of PSP1 with RNA, mediated by the RRM motifs, as documented above. In addition, we observe that PAGFP-PSP1 moves much more rapidly within the nucleoplasm outside of either paraspeckles or nucleoli (unpublished data). Within the detection limits of this assay there was no difference in the rate of movement of PAGFP-PSP1 throughout the nucleoplasm in regions without paraspeckles or nucleoli before or after ActD treatment (unpublished data). We infer that when PSP1 localizes to either paraspeckles or perinucleolar caps it makes additional molecular interactions that reduce its mobility as compared with diffusion of PSP1 through other nucleoplasmic regions.

DISCUSSION

This study describes experiments that analyze the molecular interactions and localization patterns of paraspeckle proteins. We show that PSP1 heterodimerizes with a subset of the total cellular pool of p54nrb and that the ability to form this interaction is required for its targeting to paraspeckles and perinucleolar caps. In addition, RNA binding is also required for the paraspeckle targeting of PSP1. These different requirements for localization are reflected in the different

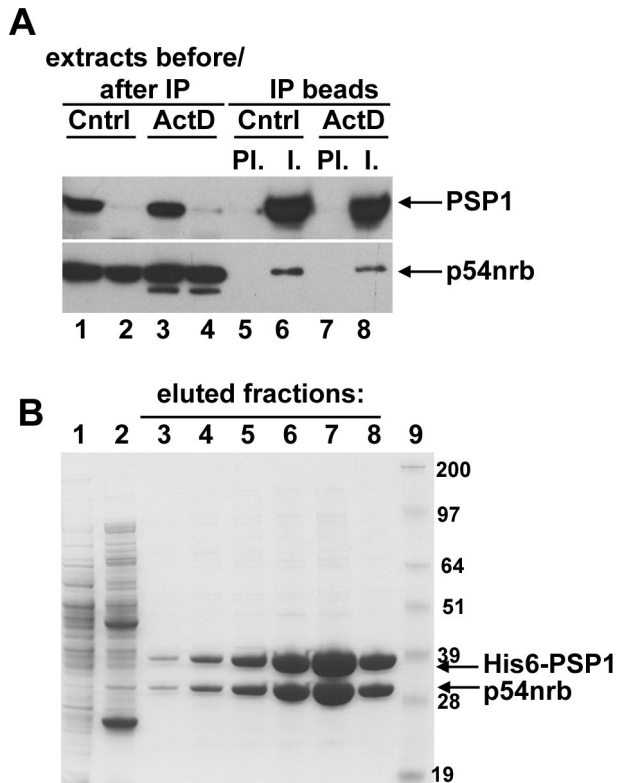


Figure 8. PSP1 and p54nrb associate when RNA Pol II transcription is inhibited and form a heterodimer *in vitro*. (A) Western blot of HeLa nuclear extract before (lanes 1 and 3) and after IP (lanes 2 and 4) of endogenous PSP1 and its partner proteins (lanes 1–4) and the immunoprecipitated proteins bound to the beads (lanes 5–8). Extracts were prepared from control HeLa cells (lanes 1, 2, 5, and 6) and HeLa cells treated with ActD (lanes 3, 4, 7, and 8). To monitor that ActD treatment was effective, the relocalization of PSP1 to perinucleolar caps was checked before cell lysis. Either preimmune serum (lanes 5 and 7) or PSP1 Ab2 were used for IP (lanes 6 and 8). The protein extracts and washed beads were subjected to SDS-PAGE, transferred to nitrocellulose and Western blotted with either anti-PSP1 (top panel), or anti-p54nrb (bottom panel). The signal was detected with ECL plus. (B) Lysates of *E. coli* transformed with pETDuet-His₆-PSP1(61–328)/p54nrb(75–313) and induced for protein expression (see *Materials and Methods*) were loaded on Ni-agarose, the flow-through was collected (lane 1), the column was washed (lane 2), and fractions were eluted with increasing imidazole (lanes 3–8). Samples were subjected to SDS-PAGE and stained with Colloidal blue. Molecular weight markers, lane 9 (kDa).

dynamics, sensitivity to RNase treatment and relationship to RNA Pol II transcription of PSP1 at paraspeckles and perinucleolar caps.

Once paraspeckles are formed they remain largely unchanged throughout the cell cycle and only disappear once daughter nuclei form in telophase. After a 20–30-min accumulation in perinucleolar caps, PSP1 is then distributed diffusely in the nucleoplasm for ~2 h before the reappearance of paraspeckles. Given that RNA Pol II transcription is active during this 2-h period (Prasanth *et al.*, 2003), why is there a significant delay between the commencement of RNA Pol II transcription and the appearance of paraspeckles? One possibility is that large amounts of RNA Pol II transcripts have to build up in the nucleus before paraspeckles form; another is that the absence of a product whose appearance is dependent on expression of one or more RNA Pol II transcripts causes the delay. In the latter case, the

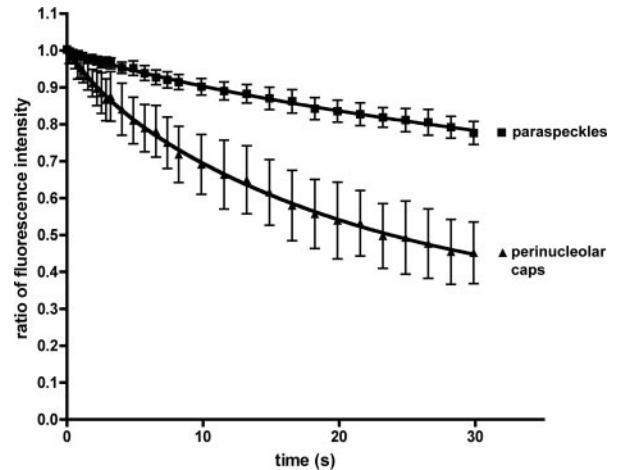


Figure 9. Differing dynamics of fluorescent-PSP1 in paraspeckles versus perinucleolar caps. The graph shows the combined data (mean and 95% confidence interval) of the loss of photoactivated paGFP-PSP1 protein from paraspeckles and perinucleolar cap structures in 30 different HeLa cells transiently expressing PA-GFP-PSP1 (see *Materials and Methods*). For each time point, the background (preactivation) fluorescence was subtracted, and the resultant value was expressed as a ratio of the first activated fluorescence value (i.e., value at 0 s). The data points are connected by a curve of best fit (2-phase exponential decay).

delay in paraspeckle formation might reflect the time taken for various nuclear export/import steps and/or processing of these products. Overall, these data suggest paraspeckles, despite being dependent on RNA for their integrity, are not associated directly with early RNA Pol II transcription events. This fits with the fact that they do not colocalize with sites of transcription as defined by Br-UTP incorporation (Fox *et al.*, 2002).

Paraspeckle proteins redistribute and instead accumulate at perinucleolar caps once RNA Pol II transcription is inhibited (Fox *et al.*, 2002; Shav-Tal *et al.*, 2005). Here we show that PSP1 perinucleolar caps form transiently in telophase before transcription has recommenced after cell division. This PSP1 perinucleolar cap localization, previously only seen with drug treatment, thus occurs naturally with each cell cycle. Others have observed similar transient perinucleolar cap localization of SR-protein splicing factors at telophase (Nicol *et al.*, 2000; Bubulya *et al.*, 2004). Bubulya *et al.* (2004) speculate that the transient segregation of SR factors at perinucleolar caps establishes specific protein-protein interactions before transcription starting in the daughter nuclei. Further, only the hypophosphorylated forms of the SR proteins were detected in these transient caps. This is interesting as both p54nrb and PSF are phosphorylated during mitosis (Shav-Tal *et al.*, 2001; Proteau *et al.*, 2005). Therefore the transient accumulation of paraspeckle proteins within perinucleolar caps at telophase may facilitate the association of paraspeckle proteins with different phospho-states.

Paraspeckles often appear to distribute nonrandomly throughout the nucleoplasm in clusters (for example, Figure 3A). This could arise if they are associated with specific chromosomal domains. However, none of our data show a direct interaction between paraspeckles and chromatin, either in interphase or in mitosis. Instead, our data suggest that paraspeckles are RNA-protein structures, as they are disrupted by RNase A treatment and because PSP1 requires a RRM able to bind RNA to be targeted to paraspeckles.

Thus paraspeckles may form as a result of RNA-protein interactions between paraspeckle proteins and RNA Pol II transcripts generated from specific loci. For example, this may be akin to nuclear stress bodies (nSB), which form around specific satellite repeat RNA molecules that are transcribed under heat shock conditions (Rizzi *et al.*, 2004). Paraspeckles may arise in a similar way, except their RNA component is transcribed under normal conditions, rather than after heat shock. Interestingly, some proteins are targeted to nSB via their ability to bind RNA (e.g., HAP and SF2/ASF), whereas others are not (e.g., HSF1 and hyperacetylated histones). Thus, in order to better understand paraspeckle function, it will be critical to identify the gene loci adjacent to paraspeckles and the transcripts that are generated from them. This is the subject of our current investigations.

All paraspeckle proteins contain two classical RRM motifs. Here we have shown that a functioning RRM is critical for the targeting of PSP1 to paraspeckles. CFI(m)68, a protein with partial paraspeckle localization, also requires the domain responsible for RNA binding in order to localize correctly in the nucleoplasm (Dettwiler *et al.*, 2004). Interestingly, the CFI(m)68 domain that mediates RNA binding is not the RRM motifs, but rather the region C-terminal to this, and the RRM motifs themselves are dispensable for correct localization of CFI(m)68 (Dettwiler *et al.*, 2004). It will be interesting to determine if the other proteins also require RNA-binding, either via RRM motifs or otherwise, for paraspeckle localization.

PSF and p54nrb are well-characterized proteins that have been implicated in multiple nuclear processes, in many cases acting as a heterodimer (Zhang *et al.*, 1993; Peng *et al.*, 2002). Here, we show that PSP1 forms a complex with a subset of the total cellular pool of p54nrb *in vivo* and heterodimerizes with p54nrb *in vitro*. Thus it is likely that any given p54nrb molecule heterodimerizes either with PSP1 or PSF with the majority of p54nrb heterodimerizing with PSF. Given this, why has PSP1 not been found in any p54nrb complexes previously identified? Either PSP1 is present, but in lower amounts than p54nrb and PSF and therefore not readily detected, or, p54nrb/PSP1 has not been specifically pulled down with any reagents used thus far. The *C. tentans* homolog of the PSP1/PSF/p54nrb family, Hrp65, self-associates through its DBHS domain (comprising the two RRM motifs and the region C-terminal containing the coiled coil domain) (Kiesler *et al.*, 2003). Consistent with this, our data show that PSP1 heterodimerizes with p54nrb via its coiled coil domain, contained within its DBHS domain. Similarly, the DBHS domain of p54nrb is required for its interaction with PSF (Zhang *et al.*, 1993; Peng *et al.*, 2002). Because both p54nrb and PSF contain similar DBHS domains, it is curious that PSP1 only heterodimerizes *in vivo* with p54nrb, and not with PSF. We note that PSP1 and PSF can co-IP if they are both overexpressed (Myojin *et al.*, 2004); however, our data suggest that the endogenous proteins do not interact in HeLa cells. Similarly, although overexpressed YFP-PSP1 can homodimerize with endogenous PSP1, our data also suggest the bulk of endogenous PSP1 exists as a p54nrb heterodimer. Clearly there must exist additional determinants *in vivo* for choice of heterodimerization partner within this family of proteins.

Unlike PSP1, which can utilize either one of its two RRMs to be targeted to paraspeckles, only the second RRM of PSF is sufficient to target PSF to subnuclear foci (Dye and Patton, 2001). Based on our data, it is likely these foci are paraspeckles. These different RRM requirements may reflect subtle differences in the functions of PSP1/p54nrb and PSF/p54nrb

at paraspeckles. Moreover, this suggests that the p54nrb partner, rather than p54nrb itself, may direct the RNA-binding specificity of the heterodimer at paraspeckles. We hypothesize that PSP1 and PSF could each target p54nrb to different substrates, in a manner analogous to Protein Phosphatase 1 (PP1) targeting subunits that direct a common catalytic component to different subcellular locations to act on different substrates (Cohen, 2002).

One of the most intriguing functions ascribed to p54nrb and PSF is the ability to bind and retain double-stranded, hyper-A-to-I-edited RNA within the nucleus (Zhang and Carmichael, 2001). Given that both PSF and p54nrb are found enriched in paraspeckles, that paraspeckles form dependent on RNA Pol II transcription and that paraspeckles are dependent on RNA for their structural integrity, one possibility is that paraspeckles are sites of nuclear retention of edited dsRNAs. If this is the case, it is interesting that PSP1 was not detected in the complex of proteins bound to edited dsRNA; either it was not present or was below the detection threshold of this experiment. Regardless, it will be interesting to determine if PSP1/p54nrb can bind hyperedited dsRNA, making paraspeckles a candidate location for nuclear hyperedited RNA.

It has been postulated that p54nrb and PSF carry out their many nuclear functions depending on their phosphorylation status and intranuclear location (Shav-Tal and Zipori, 2002). Paraspeckles therefore likely represent the site of a specific subset of the functions of these molecules. Moreover, the existence of PSP1 suggests another mechanism for the control of these myriad processes: namely that the choice of p54nrb partner may affect its function. Given this, it will be important to determine if PSP1/p54nrb carries out a novel function, or rather is implicated in the known functions of p54nrb. To this end, we have shown that we can efficiently express recombinant PSP1 and p54nrb as a stable heterodimer in *E. coli*. Future experiments will focus on characterizing the properties, structure and RNA-binding specificity of the PSP1/p54nrb heterodimer to determine the role played *in vivo* at paraspeckles. Delineating the RNA-binding specificity of the PSP1/p54nrb heterodimer will also address our hypothesis that the timing of paraspeckle formation is dictated by the synthesis of specific RNA Pol II transcripts following cell division.

ACKNOWLEDGMENTS

We thank Yun Wah Lam, Sam Swift, Laura Trinkle-Mulcahy, and Paul Andrews for help with microscopy and other members of the Lamond laboratory for helpful comments on the manuscript. A.H.F. is supported by a Caledonian Research Foundation Fellowship, C.S.B. by a BBSRC Fellowship, and A.I.L. by a Wellcome Trust Fellowship.

REFERENCES

- Andersen, J. S., Lyon, C. E., Fox, A. H., Leung, A.K.L., Lam, Y. W., Steen, H., Mann, M., and Lamond, A. I. (2002). Directed proteomic analysis of the human nucleolus. *Curr. Biol.* 12, 1–11.
- Auboeuf, D., Dowhan, D. H., Li, X., Larkin, K., Ko, L., Berget, S. M., and O'Malley, B. W. (2004). CoAA, a nuclear receptor coactivator protein at the interface of transcriptional coactivation and RNA splicing. *Mol. Cell. Biol.* 24, 442–453.
- Brown, S. A., Ripperger, J., Kadener, S., Fleury-Olela, F., Vilbois, F., Rosbash, M., and Schibler, U. (2005). PERIOD1-associated proteins modulate the negative limb of the mammalian circadian oscillator. *Science* 308, 693–696.
- Bubulya, P. A., Prasanth, K. V., Deerinck, T. J., Gerlich, D., Beaudouin, J., Ellisman, M. H., Ellenberg, J., and Spector, D. L. (2004). Hypophosphorylated SR splicing factors transiently localize around active nucleolar organizing regions in telophase daughter nuclei. *J. Cell Biol.* 167, 51–63.

- Carmo-Fonseca, M., Ferreira, J., and Lamond, A. I. (1993). Assembly of snRNP-containing coiled bodies is regulated in interphase and mitosis—evidence that the coiled body is a kinetic nuclear structure. *J. Cell Biol.* *120*, 841–852.
- Cohen, P. T. (2002). Protein phosphatase 1—targeted in many directions. *J. Cell Sci.* *115*, 241–256.
- Dettwiler, S., Aringhieri, C., Cardinale, S., Keller, W., and Barabino, S. M. (2004). Distinct sequence motifs within the 68-kDa subunit of cleavage factor Im mediate RNA binding, protein-protein interactions, and subcellular localization. *J. Biol. Chem.* *279*, 35788–35797.
- Dye, B. T., and Patton, J. G. (2001). An RNA recognition motif (RRM) is required for the localization of PTB-associated splicing factor (PSF) to subnuclear speckles. *Exp. Cell Res.* *263*, 131–144.
- Fox, A. H., Lam, Y. W., Leung, A., Lyon, C. E., Andersen, J. S., Mann, M., and Lamond, A. I. (2002). Paraspeckles: a novel nuclear domain. *Curr. Biol.* *12*, 13–25.
- Fribourg, S., Gatfield, D., Izaurralde, E., and Conti, E. (2003). A novel mode of RBD-protein recognition in the Y14-Mago complex. *Nat. Struct. Biol.* *10*, 433–439.
- Ishitani, K., Yoshida, T., Kitagawa, H., Ohta, H., Nozawa, S., and Kato, S. (2003). p54nrb acts as a transcriptional coactivator for activation function 1 of the human androgen receptor. *Biochem. Biophys. Res. Commun.* *306*, 660–665.
- Iwasaki, T., Chin, W. W., and Ko, L. (2001). Identification and characterization of rrm-containing coactivator activator (coa) as trbp-interacting protein, and its splice variant as a coactivator modulator (coam). *J. Biol. Chem.* *276*, 33375–33383.
- Jones, K. R., and Rubin, G. M. (1990). Molecular analysis of no-on-transient A, a gene required for normal vision in *Drosophila*. *Neuron* *4*, 711–723.
- Kiesler, E., Miralles, F., Farrants, A. K., and Visa, N. (2003). The Hrp65 self-interaction is mediated by an evolutionarily conserved domain and is required for nuclear import of Hrp65 isoforms that lack a nuclear localization signal. *J. Cell Sci.* *116*, 3949–3956.
- Leung, A. K., Gerlich, D., Miller, G., Lyon, C., Lam, Y. W., Lleres, D., Daigle, N., Zomerdijk, J., Ellenberg, J., and Lamond, A. I. (2004). Quantitative kinetic analysis of nucleolar breakdown and reassembly during mitosis in live human cells. *J. Cell Biol.* *166*, 787–800.
- Lisbin, M. J., Gordon, M., Yannoni, Y. M., and White, K. (2000). Function of RRM domains of *Drosophila melanogaster* ELAV: Rnp1 mutations and rrm domain replacements with ELAV family proteins and SXL. *Genetics* *155*, 1789–1798.
- Miralles, F., Ofverstedt, L. G., Sabri, N., Aissouni, Y., Hellman, U., Skoglund, U., and Visa, N. (2000). Electron tomography reveals posttranscriptional binding of pre-mRNPs to specific fibers in the nucleoplasm. *J. Cell Biol.* *148*, 271–282.
- Miralles, F., and Visa, N. (2001). Molecular characterization of Ct-hrp65, identification of two novel isoforms originated by alternative splicing. *Exp. Cell Res.* *264*, 284–295.
- Myojin, R., Kuwahara, S., Yasaki, T., Matsunaga, T., Sakurai, T., Kimura, M., Uesugi, S., and Kurihara, Y. (2004). Expression and functional significance of mouse paraspeckle protein 1 on spermatogenesis. *Biol. Reprod.* *71*, 926–932.
- Nicol, S. M., Causevic, M., Prescott, A. R., and Fuller-Pace, F. V. (2000). The nuclear DEAD box RNA helicase p68 interacts with the nucleolar protein fibrillarin and colocalizes specifically in nascent nucleoli during telophase. *Exp. Cell Res.* *257*, 272–280.
- Peng, R., Dye, B. T., Perez, I., Barnard, D. C., Thompson, A. B., and Patton, J. G. (2002). PSF and p54nrb bind a conserved stem in U5 snRNA. *RNA* *8*, 1334–1347.
- Percipalle, P., Fomproix, N., Kylberg, K., Miralles, F., Bjorkroth, B., Daneholt, B., and Visa, N. (2003). An actin-ribonucleoprotein interaction is involved in transcription by RNA polymerase II. *Proc. Natl. Acad. Sci. USA* *100*, 6475–6480.
- Prasanth, K. V., Sacco-Bubulya, P. A., Prasanth, S. G., and Spector, D. L. (2003). Sequential entry of components of the gene expression machinery into daughter nuclei. *Mol. Biol. Cell* *14*, 1043–1057.
- Price, S. R., Evans, P. R., and Nagai, K. (1998). Crystal structure of the spliceosomal U2B′-U2A′ protein complex bound to a fragment of U2 small nuclear RNA. *Nature* *394*, 645–650.
- Proteau, A., Blier, S., Albert, A. L., Lavoie, S. B., Traish, A. M., and Vincent, M. (2005). The multifunctional nuclear protein p54nrb is multiphosphorylated in mitosis and interacts with the mitotic regulator Pin1. *J. Mol. Biol.* *346*, 1163–1172.
- Rizzi, N., Denegri, M., Chiodi, I., Corioni, M., Valgardsdottir, R., Cobiانchi, F., Riva, S., and Biamonti, G. (2004). Transcriptional activation of a constitutive heterochromatic domain of the human genome in response to heat shock. *Mol. Biol. Cell* *15*, 543–551.
- Selenko, P., Gregorovic, G., Sprangers, R., Stier, G., Rhani, Z., Kramer, A., and Sattler, M. (2003). Structural basis for the molecular recognition between human splicing factors U2AF65 and SF1/mBBP. *Mol. Cell* *11*, 965–976.
- Serin, G., Joseph, G., Ghisolfi, L., Bauzan, M., Erard, M., Amalric, F., and Bouvet, P. (1997). Two RNA-binding domains determine the RNA-binding specificity of nucleolin. *J. Biol. Chem.* *272*, 13109–13116.
- Shav-Tal, Y., Blechman, J., Darzacq, X., Montagna, C., Dye, B. T., Patton, J. G., Singer, R. H., and Zipori, D. (2005). Dynamic sorting of nuclear components into distinct nucleolar caps during transcriptional inhibition. *Mol. Biol. Cell* *16*, 2395–2413.
- Shav-Tal, Y., Cohen, M., Lapter, S., Dye, B., Patton, J. G., Vandekerckhove, J., and Zipori, D. (2001). Nuclear relocalization of the pre-mRNA splicing factor PSF during apoptosis involves hyperphosphorylation, masking of antigenic epitopes, and changes in protein interactions. *Mol. Biol. Cell* *12*, 2328–2340.
- Shav-Tal, Y., and Zipori, D. (2002). PSF and p54(nrb)/NonO—multi-functional nuclear proteins. *FEBS Lett.* *531*, 109–114.
- Zhang, W. W., Zhang, L. X., Busch, R. K., Farres, J., and Busch, H. (1993). Purification and characterization of a DNA-binding heterodimer of 52 and 100 kDa from HeLa cells. *Biochem. J.* *290*(Pt 1), 267–272.
- Zhang, Z., and Carmichael, G. G. (2001). The Fate of dsRNA in the Nucleus. A p54(nrb)-containing complex mediates the nuclear retention of promiscuously A-to-I edited RNAs. *Cell* *106*, 465–475.